JACC: CARDIOVASCULAR IMAGING
VOL. 7, NO. 11, 2014

ISSN 1936-878X/$36.00
PUBLISHED BY ELSEVIER INC.

iMAIL

LETTERS TO THE EDITOR

Multiple Simultaneous Plaque Erosion in 3 Coronary Arteries

We performed optical coherence tomography (OCT) imaging with matched histology in a 34-year-old man with history of smoking and untreated hyperlipidemia who had suffered from epigastric pain and was found dead at home. Multiple plaque erosions in 3 major coronary arteries were discovered (Figure 1).

Plaque erosion is suspected in the presence of an acute luminal thrombus that is in direct contact with the underlying intima comprising smooth muscle cells and proteoglycan with an absence of endothelial lining (1). The erosive plaques are rich in versican,

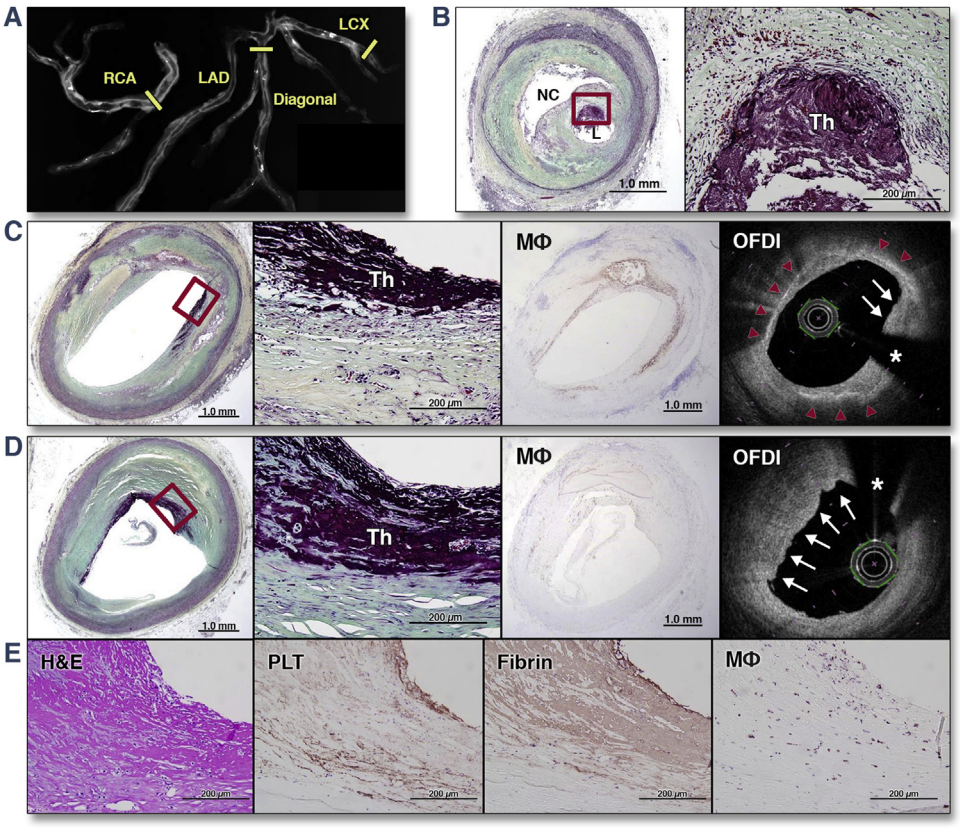

FIGURE 1 Multiple Plaque Erosions in 3 Major Coronary Arteries

(A) Postmortem radiography showed focal mild calcification in all major coronary arteries. **(B)** Histologic examination showed the left circumflex artery (LCX) with a nonocclusive platelet-rich organizing thrombus (Th) with underlying late fibroatheroma. **(C)** The right coronary artery (RCA) showed a luminal fibrin-rich organizing thrombus with an underlying late fibroatheroma. **(D)** The diagonal branch artery also showed a luminal fibrin-rich organizing thrombus with an underlying pathological intimal thickening. High-power images from **boxes** in **C** and **D** are shown. Fibrin-rich thrombus with a few inflammatory cells are seen on the luminal surface. Corresponding macrophage (MΦ) stain and optical frequency domain imaging images (OFDI) (Terumo, Tokyo, Japan) are depicted. Moderate macrophage infiltration is seen around the circumference of the vessel **(red arrows)**; however, the culprit site **(white arrows)** is devoid of macrophages in the RCA. Note the absence of macrophage in the diagonal branch (macrophages stained section of **D**). OFDI showed luminal surface irregularity with minimal attenuation because the thrombus had focal areas of platelets interspersed by large areas of fibrin in the RCA and the diagonal branch **(white arrows),** and a bright layer with attenuation **(red arrowheads)** indicates presence of macrophages in RCA **(C). (E)** Serial sections at high-power stained by hematoxylin and eosin (H&E), platelet ([PLT] CD61), fibrin (fibrin II), and macrophage (CD68) stained images from the box in **D** are shown. Platelet stains **(brown)** show few superficial and interspersed platelets with a predominance of fibrin (**brown**, adjacent section) and rare macrophage infiltration **(brown)**. *Placement of the guidewire. L = lumen; LAD = left anterior descending; NC = necrotic core.

hyaluronan, and type III collagen, unlike rupture or stable plaques, which are rich in type I collagen (2). The erosion lesions are more often eccentric and infrequently calcified; they show minimal inflammation with a few or absent macrophages and T-lymphocytes (2). The media underneath plaque erosions are similar to plaques with mild stenosis, rich in smooth muscle cell actin, which is also highly expressed in intimal smooth muscle cells in erosions. Plaque erosions often show negative remodeling. It is likely that spasm may play an important role in plaque erosion.

Plaque erosion accounts for 25% to 35% of coronary thrombi in patients dying of acute myocardial infarction and/or sudden coronary death (1). Plaque erosions occur in individuals with relatively low total cholesterol, higher high-density lipoprotein cholesterol, and low total cholesterol /high-density lipoprotein cholesterol ratio as compared to plaque rupture (1). Consistently, smoking is an important risk factor of plaque erosion in men and women dying of sudden coronary death (1). Also, plaque erosions are observed with greater frequency in women, less percentage of stenosis, less calcification, and less plaque burden (1). Plaque erosion accounts for over 80% of thrombi in women <50 years of age, with less frequency in older women (>50 years). Severe narrowing (>75% cross-sectional area narrowing) is only observed in 40% of plaque erosions whereas 48% show 51% to 75% luminal narrowing and only 12% of erosions have <50% narrowing. Necrotic core area follows the same trends with the least number of areas seen in those with less stenosis, and macrophage infiltration in similar irrespective of the degree of stenosis.

At the time of presentation, 88% of plaque erosions show healing—nuclear breakdown, proliferation of smooth muscle and endothelial cells—as compared to 54% of ruptured plaques ($p < 0.0001$). Thrombus is almost always organizing in less stenotic lesions as compared to severely stenotic erosions, which show the least thrombus organization. In 96% of cases, plaque erosion is observed at a single site within the coronary tree, whereas 4% of cases show multiple sites of erosion. The underlying plaque morphology consists of either pathological intimal thickening or fibroatheroma (pathological intimal thickening 16%, early fibroatheroma 50%, and late fibroatheroma 34%); the media show intact internal elastic lamina and external elastic lamina in 32% of cases, focally disrupted IEL (from inflammation and angiogenesis) in 52%, and, uncommonly, both IEL and EEL disrupted in 16% of cases. The majority of erosion lesions show no calcification (56%); microcalcification is observed in 40%, whereas fragmented and sheets of calcification are seen in 2%, each. Inflammation is usually absent or minimal in 68% of cases within the transition zone between thrombus and underlying plaque and mild in 32%. Furthermore, inflammation at the adventitial medial border is absent or minimal in 34%, mild in 50%, and rarely moderate or severe in 18% of cases (14% and 4%, respectively) (1).

Until recently it was not possible to identify plaque erosion in living patients. With the advent of OCT, it has become possible to differentiate the acute coronary events resulting from the underlying plaques with ruptured fibrous caps or intact fibrous caps (3). A definite diagnosis of plaque erosion requires the presence of an acute luminal thrombus with a nonruptured visualized plaque (4). Probable OCT erosion was defined as luminal surface irregularity or attenuation of underlying plaque by thrombus without superficial lipid or calcification at the adjacent proximal or distal sections. OCT-defined plaque erosion occurs in 31% of patients presenting with acute coronary syndromes. It has been proposed that the acute event associated with intact fibrous caps may not need to be treated with balloon dilation or stent implantation if the lumen is not critically compromised (5). These patients may be left alone after the thrombus aspiration on dual antiplatelet agents. However, no distinct plaque morphologic features of erosion-prone plaques have been identified. These findings allude to the necessity to reconsider differences in the mechanism of thrombosis between erosion versus rupture, and that perhaps different strategies are required for their treatment because in only 40% of cases is severe stenosis identified.

Kazuyuki Yahagi, MD
Roya Zarpak, MS
Kenichi Sakakura, MD
Fumiyuki Otsuka, MD, PhD
Robert Kutys, MS
Elena Ladich, MD
David R. Fowler, MD
Michael Joner, MD
Renu Virmani, MD*

*CVPath Institute, Inc.
19 Firstfield Road
Gaithersburg, Maryland 20878
E-mail: rvirmani@cvpath.org

http://dx.doi.org/10.1016/j.jcmg.2014.08.005

Please note: Dr. Sakakura is supported by a research fellowship from the Banyu Life Science Foundation International; and has received speaking honoraria from Abbott Vascular, Boston Scientific, and Medtronic Cardiovascular. Dr. Joner has consulted for Biotronik and Cardionovum; and has received

speaking honorarium from Abbott Vascular, Biotronik, Medtronic, and St. Jude Medical. Dr. Virmani receives research support from Abbott Vascular, Bio-Sensors International, Biotronik, Boston Scientific, Medtronic, MicroPort Medical, OrbusNeich Medical, SINO Medical Technology, and Terumo Corporation; has speaking engagements with Merck; receives honoraria from Abbott Vascular, Boston Scientific, Lutonix, Medtronic, and Terumo Corporation; and consults for 480 Biomedical, Abbott Vascular, Medtronic, and W. L. Gore. All other authors have reported that they have no relationships relevant to the contents of this paper to disclose.

REFERENCES

1. Burke AP, Farb A, Malcom GT, Liang Y, Smialek J, Virmani R. Effect of risk factors on the mechanism of acute thrombosis and sudden coronary death in women. Circulation 1998;97:2110–6.

2. Kolodgie FD, Burke AP, Farb A, et al. Differential accumulation of proteoglycans and hyaluronan in culprit lesions: insights into plaque erosion. Arterioscler Thromb Vasc Biol 2002;22:1642–8.

3. Ozaki Y, Okumura M, Ismail TF, et al. Coronary CT angiographic characteristics of culprit lesions in acute coronary syndromes not related to plaque rupture as defined by optical coherence tomography and angioscopy. Eur Heart J 2011;32:2814–23.

4. Jia H, Abtahian F, Aguirre AD, et al. In vivo diagnosis of plaque erosion and calcified nodule in patients with acute coronary syndrome by intravascular optical coherence tomography. J Am Coll Cardiol 2013;62:1748–58.

5. Prati F, Uemura S, Souteyrand G, et al. OCT-based diagnosis and management of STEMI associated with intact fibrous cap. J Am Coll Cardiol Img 2013;6:283–7.

Flare Spots in Intravascular Optical Coherence Tomography Images of Bioabsorbable Stents

Flare spots (**Figures 1A and 1B**) are observed in intravascular optical coherence tomography (IVOCT) images of bioabsorbable stent struts in patients and have no analog in metallic stents. Gutiérrez-Chico et al. (1) proposed that flare spots were located at hinge points where the highest strain is experienced during deployment, suggesting that they represent micro-crazes (fine lines) in the polymer. Nonetheless, the mechanism for the presence of flare spots in IVOCT images, and the large variation in their appearance where no two are alike, is not known. In this study, micro-CT and IVOCT images of a bioabsorbable stent deployed in a cylindrical phantom blood vessel were coregistered and compared in order to investigate the underlying mechanism for presence of flare spots in IVOCT images.

A 3-mm lumen diameter phantom vessel was made out of polydimethylsiloxane with elastic properties comparable to that of arteries. Titanium dioxide was added to polydimethylsiloxane to simulate the light-scattering properties of the arterial wall. A 3.0 × 18 Absorb stent (Abbott Vascular, Santa Clara, California) was deployed within the phantom vessel at 16-atm pressure with a balloon while submerged in a water bath at body temperature (37°C) to minimize any structural changes to the polymer. IVOCT images of the Absorb stent (**Figures 1C and 1D**) were acquired using a frequency domain IVOCT system (CorVue, Volcano Corporation, San Diego, California) while the phantom vessel was flushed with saline. The IVOCT catheter was pulled back at a slow speed of 1.5 mm/s over a 15-mm length of vessel recording at a rate of 30 frames/s. After stent deployment and IVOCT imaging, micro-CT images of the phantom vessel at resolution of 6 μm were recorded as a gold image standard. Each recorded IVOCT image was registered to a sequence of 8 micro-CT images due to the spiral pattern associated with a pullback and relatively larger longitudinal spacing between IVOCT images. **Figure 1** illustrates 2 successive IVOCT images (**Figures 1C and 1D**) along with the corresponding coregistered micro-CT images (**Figures 1E and 1F**). The change in appearance of groups of struts (indicated with green and yellow ovals) can be observed in successive IVOCT and micro-CT images. From the micro-CT image sequence (**Figures 1E and 1F**), adjacent struts are observed to merge (separate) at the arterial side of the stent and form a micro-sized gap at the vessel wall, with a different appearance at every gap. Flare spots in the IVOCT images are only generated when gaps appear in the micro-CT images on the arterial side.

The micro-CT dataset was used to create a 3-dimensional representation of the entire stent demonstrating that micro-crazes are formed on the arterial side of the stent and therefore result in micro-gaps at the vessel wall. There were 2 types of crazing, which correspond to locations where 2 or 3 struts merge (separate). During a pullback, the IVOCT beam propagates through the vessel lumen, where portions of light reflect from and transmit across the strut edge. Light reflected from the strut edge forms an outline of the outer surface of the strut in IVOCT images. When the IVOCT beam enters a gap region with micro-crazes, reflections at the gap boundary occur before light returns to the catheter. The reflections at gap boundaries produce flare spots of higher intensity inside struts in IVOCT images (**Figure 1G**). Because each crazing site is different at every hinge point, as demonstrated by the micro-CT images (**Figures 1E and 1F**), the pattern of light reflections is expected to vary, which is consistent with the observation that no two flare spots appear identical in recorded IVOCT images.

In conclusion, we have completed imaging experiments of an Absorb stent deployed in a phantom vessel to investigate the origin of flare spots observed in IVOCT images of bioabsorbable stents. Flare spots observed in IVOCT images correspond to gaps observed in micro-CT images formed by micro-crazes